European Journal of Immunology

Myosin 1g regulates cytoskeleton plasticity, cell migration, exocytosis, and endocytosis in B lymphocytes

José L. Maravillas-Montero[*1], *Orestes López-Ortega*[*1], *Genaro Patiño-López*[2] *and Leopoldo Santos-Argumedo*[1]

[1] Departamento de Biomedicina Molecular, Centro de Investigación y de Estudios Avanzados del Instituto Politécnico Nacional, Ciudad de México, México
[2] Experimental Immunology Branch, National Cancer Institute, National Institutes of Health, Bethesda, MD, USA

Myosin 1g (Myo1g) is a hematopoietic-specific myosin expressed mainly by lymphocytes. Here, we report the localization of Myo1g in B-cell membrane compartments such as lipid rafts, microvilli, and membrane extensions formed during spreading. By using Myo1g-deficient mouse B cells, we detected abnormalities in the adhesion ability and chemokine-induced directed migration of these lymphocytes. We also assessed a role for Myo1g in phagocytosis and exocytosis processes, as these were also irregular in Myo1g-deficient B cells. Taken together, our results show that Myo1g acts as a main regulator of different membrane/cytoskeleton-dependent processes in B lymphocytes.

Keywords: B lymphocyte · Chemotaxis · Cytoskeleton · Exo-endocytosis · Myosin

Additional supporting information may be found in the online version of this article at the publisher's web-site

Introduction

Myosin I refers to a class of single-headed and actin-dependent molecular motors, which regulates a number of cellular functions, including intracellular transport, formation of cell-surface projections, regulation of the cytoskeleton, and regulation of membrane-related events, which includes exocytosis, endocytosis, and phagocytosis [1–3].

Members of myosin I family contain a single heavy chain of 110–140 kDa [4, 5], are monomeric, and do not form filaments unlike muscular/conventional myosin II. The single heavy chain is divided into the head (or motor), neck, and tail domains. The motor domain contains the ATP-binding (where ATP is adenosine triphosphate) site and the actin-binding site. This domain is followed by the neck domain, which is involved in the binding of myosin light chains; molecules identified as calmodulin in vertebrate and yeast class I myosins [6]. Following the neck domain is the C-terminal tail region, which is enriched in basic residues and is involved in the binding of membrane phosphoinositides [7, 8]. In humans and mice, eight different genes encode the eight heavy chains of class I myosins and are named Myo1a to Myo1h [2].

Myosin 1g (Myo1g) is a vertebrate class I myosin, which is highly represented in leukocytes, according to microarray databases [9–11]. Immunoblot analyses of different tissues and cell lines recently identified this protein as being an exclusively hematopoietic motor protein [12, 13].

Mass spectrometric proteomic profiling of lymphocyte proteins indicates that Myo1g is the most abundant class I myosin

Correspondence: Dr. Leopoldo Santos-Argumedo
e-mail: lesantos@cinvestav.mx

*These authors contributed equally to this work.

expressed by T lymphocytes [13]. Immunofluorescence assays showed that Myo1g localizes to the plasma membrane linked to phosphatidylinositol 4,5-bisphosphate and phosphatidylinositol 3,4,5-triphosphate [14], is particularly enriched at cell-surface microvilli, and associates in an ATP-releasable manner to the actin cytoskeleton [12, 13]. In addition to its localization pattern, it has been proposed that this molecular motor may play a role in regulating cell membrane deformation, according to experiments that demonstrate a decreased elasticity of siRNA Myo1g-depleted T cells [12].

Interestingly, Myo1g has also been found associated with cell structures such as lipid rafts in late endosomes of baby hamster kidney cells [15], in endosomes containing lipid rafts in human T lymphocytes [16], associated with MCF7 cell lysosomes, and exosomes secreted by T lymphocytes stimulated with PHA plus IL-2 [17].

As described in our previous work, Myo1g is also present and abundant in B lymphocytes [13, 18]; however, its function(s) in these cells is not known. In experiments where Myo1c, another closely related myosin expressed by B cells, has been knocked down, we observed defects in lymphocyte migration and cytoskeleton rearrangements during cell spreading [18]. Thus, it is possible that Myo1g could also participate in these processes by regulating the membrane dynamics. Therefore, in this study we analyzed how the absence of Myo1g affects the B-cell cytoskeleton and plasma membrane dynamics, focusing in the adhesion, cell migration, endocytocis, and exocytosis.

Results

Myo1g distribution in B lymphocytes

We detected the presence of Myo1g at the microvilli of spleen B cells 48 h after LPS + IL-4 activation by confocal microscopy (Fig. 1A). In the same way, we confirmed the abundance of Myo1g in these microstructures of B cells by using a mechanical shear-off approach followed by an ultracentrifugation-based separation of microvilli from the rest of the cell. As shown in Figure 1B, Myo1g was found enriched in the membrane/microvilli fraction (MMV) when compared with the postnuclear lysate (PNL) fraction that corresponds to cell bodies.

When B cells were allowed to spread over an anti-CD44-coated surface, we observed that Myo1g was localized in typical adhesion/motility-related protrusions such as actin-dependent lamellipodia and filopodia, and was also visible at the longer highly dynamic dendrite-like protrusions (Fig. 1C, white arrowheads), which were previously characterized during spreading experiments [18, 19].

As Myo1g possesses a tail homology 1 (TH1) domain (a PH-like domain) in the tail region, it can interact directly with some plasma membrane lipids. This region has been reported to be necessary for binding phosphoinositides such as those enriched in lipid rafts [20]. With this precedent and previous data reporting the inclusion of Myo1g in lipid rafts of neutrophils [21] and human B lymphocytes [22], we looked for the presence of this protein in these membrane regions of B cells. As defined by the co-localization analysis with GM1 (Fig. 1D) and the detergent extraction followed by density-gradient isolation of lipid rafts (Fig. 1E), we confirmed that Myo1g was present in these membrane domains of B lymphocytes.

Altered spreading and adhesion responses of Myo1g-deficient B cells

Through the use of a Myo1g-deficient mouse (*Myo1g*$^{-/-}$), we were able to detect some alterations in the dynamics of cytoskeleton of B cells when this protein was absent. When we compared the anti-CD44 induced spreading of WT B cells with that of *Myo1g*$^{-/-}$ B cells, we observed a clear defect in the spreading extent of Myo1g-deficient lymphocytes (Fig. 2A). In more detailed observations, it was evident that although the two groups of lymphocytes can generate filopodia protrusions, only the WT cells develop longer membrane projections, rendering elongated cell forms during both CD44 and LFA-1-induced spreading (Fig. 2B). To quantify these differences, we determine the individual area covered by each spread lymphocyte from a total of 500 cells per group, either anti-CD44 or anti-LFA-1 coated glass slides. As depicted in Figure 2C, *Myo1g*$^{-/-}$ B cells cannot extend as much as the WT cells with the two stimuli used. Correspondingly, we also quantified this response by determining the "shape factor" that resulted from the coefficient of length and width of a given cell. Values closer to 1.0 indicate a more rounded morphology; elongation of the cells corresponds to factor values >1.0 and increases proportionally as the length of the cell increases. As is shown in Figure 2D, most of the Myo1g-deficient B cells developed a rounded spreading pattern over both CD44 and LFA-1 stimuli instead of the elongated shapes of the WT B cells.

In the spreading assays, we consistently noticed few adherent *Myo1g*$^{-/-}$ cells compared with WT cells, although equal numbers of them were used in each test. To corroborate this observation, we performed a colorimetric adhesion assay, inducing the attachment of WT and Myo1g-deficient B lymphocytes, either activated or unstimulated, over different substrates. As shown in Figure 2E, plating the different cell groups over a cationic nonspecific attachment agent, such as poly-L-lysine, did not raise differences in adhesion; however, when the lymphocytes are plated over fibronectin (ligand of CD44, β1, β3, and β5–7 integrins), agonists anti-CD44 or anti-LFA-1, we detect a significant adhesive deficit in *Myo1g*$^{-/-}$ B cells. Interestingly, when we measured the surface levels of CD44 (Fig. 2F) and LFA-1 (Fig. 2G) by flow cytometry, we detected a clear reduction in the plasma membrane expression of both molecules in activated B cells.

Slow B-cell migration in vitro and defective homing in vivo

Since alterations in adhesion forces, cell spreading and membrane tension have been reported as being responsible for defective

cell migration [23–26], we tested the ability of Myo1g-deficient B cells to migrate toward a chemokine gradient. We used CXCL13 to induce migration of resting B lymphocytes over a fibronectin-coated surface in a chemotaxis chamber. As shown in Figure 3A, we observed that cell tracks of *Myo1g*$^{-/-}$ B cells were not as extended like those from WT B cells. Analysis of the mean velocity and the path length of both groups of cells yielded a significant reduction in the velocity and total migration distance of *Myo1g*$^{-/-}$ B lymphocytes compared with that of WT B cells (Fig. 3B and C). Since the defect in cell migration could be the result of a defective expression of the CXCL13's cognate receptor, we assayed for CXCR5's presence by flow cytometry, but detected no differences between both cell groups (Supporting Information Fig. 1).

We also assessed homing of B cells to secondary lymphoid organs by intravenous adoptive transfer of a mixture of *Myo1g*$^{-/-}$ and WT spleen cells marked with different concentrations of CFSE, followed by measurement of the marked B-cell number found in inguinal lymph nodes and spleen (Fig. 3D, upper panel). There was approximately a 75% reduction in the number of *Myo1g*$^{-/-}$ B-lymphocytes in both lymph nodes and spleen with a corresponding increase of those cells in peripheral blood, after 2 h (Fig. 3D, lower panel).

The lack of Myo1g impacts the phagocytosis/exocytosis functions of B cells

Using fluorescent polystyrene beads, we observed that Myo1g is also present at the developing phagocytic cups of B cells (Fig. 4A). These data lead us to speculate that Myo1g may play a role in this process.

When we performed a phagocytosis experiment, in which we "fed" primary spleen B cells with fixed FITC-*Staphylococcus aureus*, we could detect slight differences in the quantity of bacteria ingested by WT and *Myo1g*$^{-/-}$ B lymphocytes (Fig. 4C, upper panel). These spleen cells correspond almost exclusively to the B-2 subpopulation of B lymphocytes; the other subpopulation, known as B-1, is unique for their high phagocytic rate [27,28]. Therefore, we tested B cells from the peritoneal cavity, which is 60–70% of B-1 cells [29], in the previously described experiment. As predicted, we noticed that peritoneal B cells ingest more bacteria

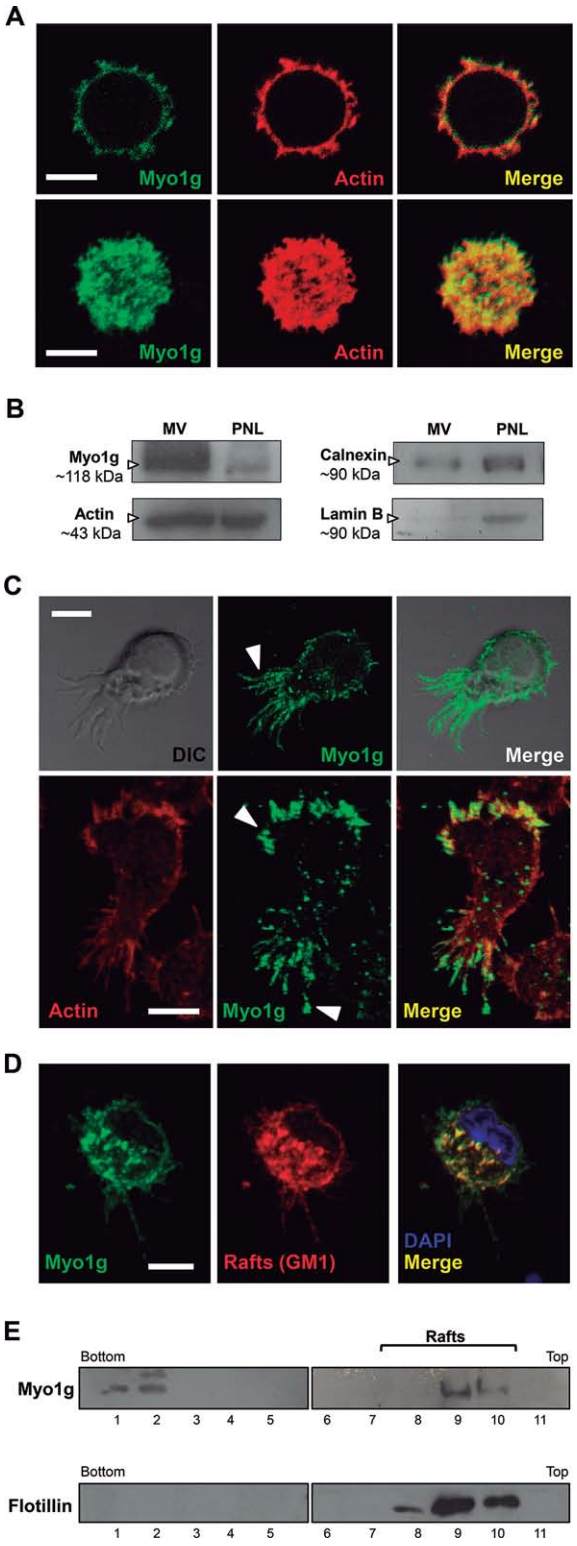

Figure 1. Distribution of Myo1g in B cells. (A) Myo1g can be found at microvilli of activated primary B cells. An optical cross-section (0.3 μm) of a B lymphocyte stained for Myo1g and F-actin for microvilli detection (top), and a 3D reconstruction of the same cell (bottom) are shown. (B) Microvilli Myo1g enrichment in B lymphocytes assessed by the shear-based procedure described in the *Materials and methods*. Equal amounts (30 μg) of total protein of the MMV and the PNL were analyzed with Western blot for detection of Myo1g, actin (enriched in MMV fraction), calnexin, and lamin B (enriched at the PNL fraction). (C) Enrichment of Myo1g at the membrane protrusions formed during B-cell spreading. A cell with dendrite-like extensions is shown with Myo1g indicated by the white arrow (top). A different lymphocyte, counterstained for F-actin, with filopodial and lamellipodial-like structures indicated by the white arrows, also showing enrichment in Myo1g (bottom). (D) Confocal projections of CD44-stimulated primary spleen B cells that were stained for Myo1g and ganglioside GM1, a marker of lipid rafts. (E) B cells were lysed using Triton X-100 at 4°C. The supernatant obtained was fractionated by sucrose density gradient to isolate buoyant detergent resistant membranes. Equivalent volumes of all fractions (20 μL) were analyzed by Western blot to detect the presence and enrichment of flotillin, as raft marker, and Myo1g. All data shown are representative of at least four independent experiments performed. Scale bars: 5 μm.

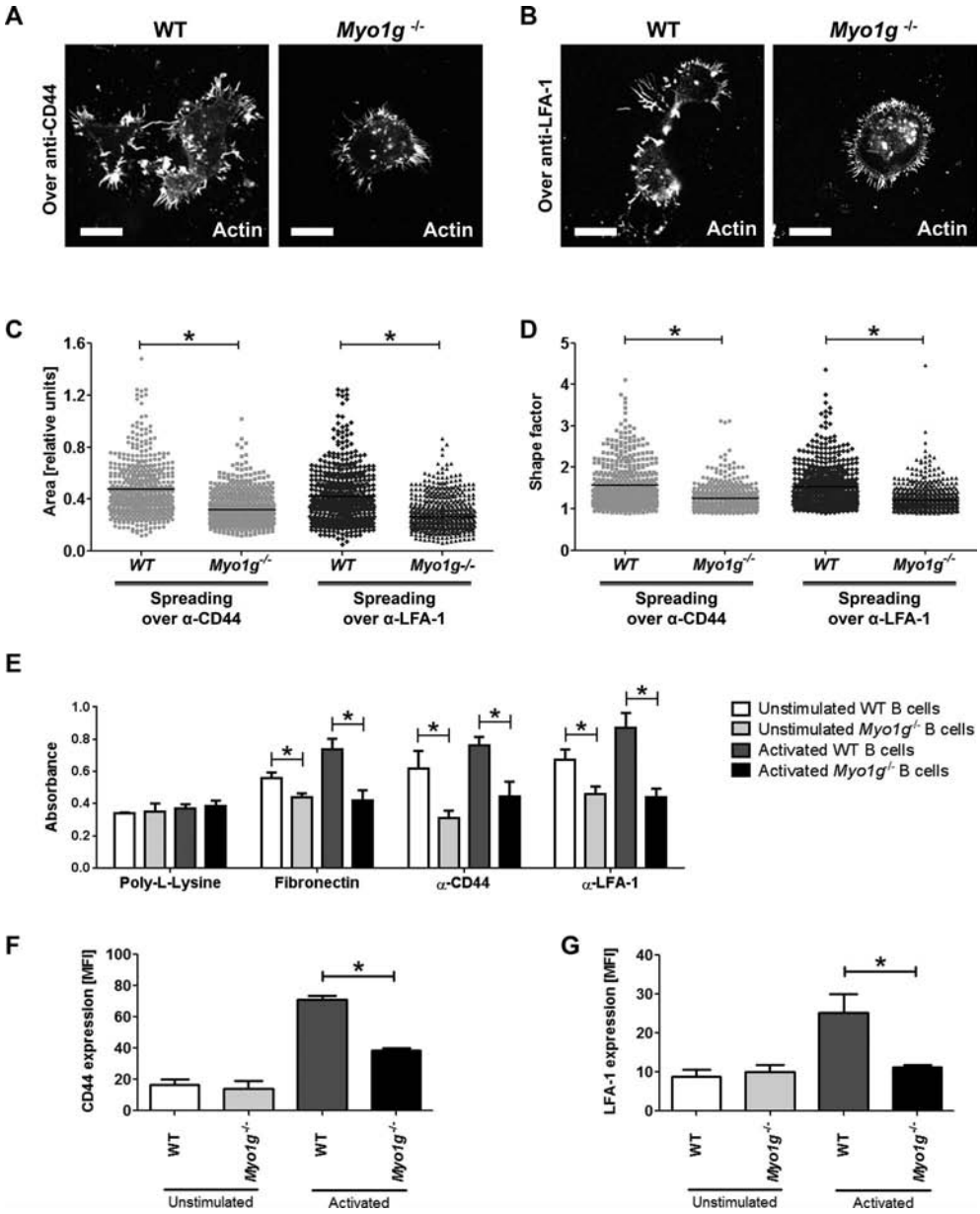

Figure 2. Myo1g is involved in B-cell spreading and adhesion. (A, B) Activated primary B cells spreading over both anti-CD44 and anti-LFA-1 were stained with tetramethylrhodamine isothiocyanate-phalloidin (TRITC) to detect F-actin. Scale bars: 5 μm. (C) Individual spread of activated B lymphocytes over either anti-CD44 or anti-LFA-1 was measured to determine its relative area comparing WT versus *Myo1g*$^{-/-}$ cells. (D) The width and length of spread lymphocytes were measured to determine "shape factor" values of each cell, which correspond to the coefficient of these two parameters. A total number of 12 fields for each condition were used to count around 20 random cells per field. Each symbol represents a single cell. (C, D) Data shown are from one experiment representative of three performed. (E) Equal numbers of resting (unstimulated) or activated B lymphocytes were placed in 96-well plates coated with fibronectin, anti-CD44, anti-LFA-1, or poly-L-lysine as control; nonadhering cells were washed away and the remaining were stained with crystal violet before lysing them. The absorbance of each sample was determined by mean + SD pooled from data of four independent experiments. (F, G) CD44 and LFA-1 surface expression was determined by flow cytometry; the MFI of resting or activated B cells from WT and *Myo1g*$^{-/-}$ mice was obtained for each sample and shown as mean + SD of three samples from one experiment representative of three performed. *$p < 0.05$, two-tailed unpaired Student's *t*-test.

than B cells isolated from spleen. The outstanding observation came when WT and *Myo1g*$^{-/-}$ B lymphocytes were tested finding that the last ones were capable of ingesting more bacteria (Fig. 4B). To measure this increased phagocytic activity, we analyzed these cells using a flow cytometry approach; as depicted in Figure 4C (lower panel), we detected an increase of at least double the MFI of ingested FITC-bacteria in *Myo1g*$^{-/-}$ B cells compared with that by WT cells.

Conversely, it has been reported that alterations in endocytosis correlate with a deficient exocytosis function [30]. As a result, we looked for defects in secreted molecules of B lymphocytes such as prolactin and TNF-α, both expressed by these cells upon activation

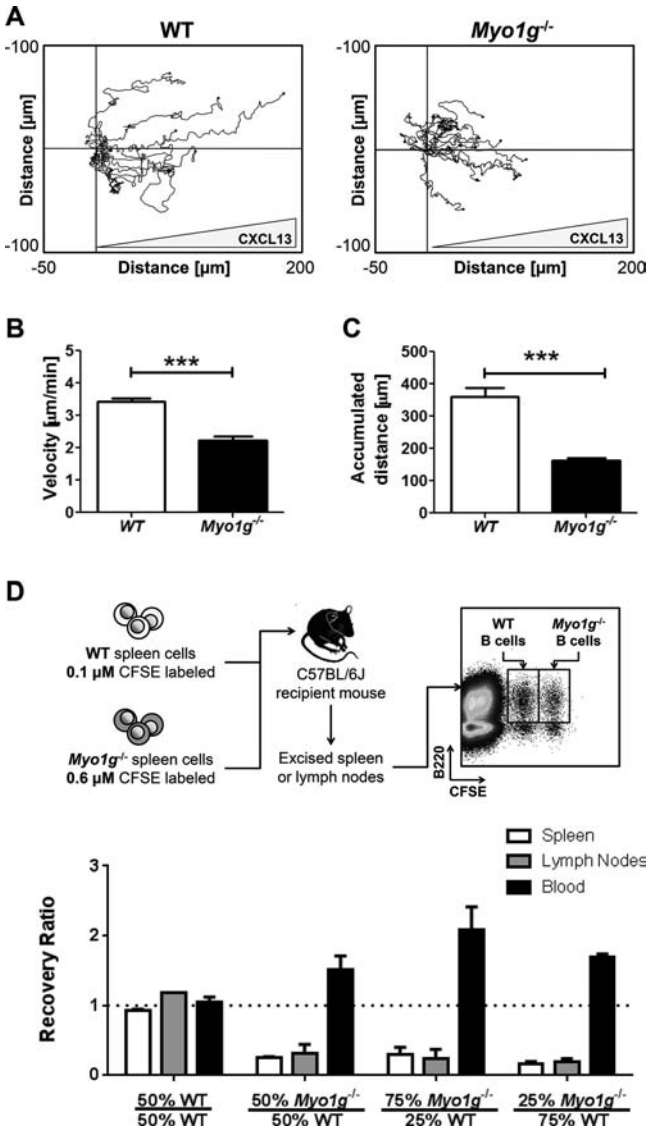

Figure 3. The lack of Myo1g affects B-cell migration. (A) Resting mouse B cells from both WT and *Myo1g*$^{-/-}$ mice were deposited in a Zigmond chemotaxis chamber under a CXCL13 gradient. Individual cell paths were traced and presented in the representative plots, from at least six independent experiments. (B) The average velocity of B cells from both genotypes migrating over the chamber was calculated and compared here. *$p < 0.0005$, two-tailed unpaired Student's *t*-test. (C) The accumulated track length of individual B cells from both genotypes migrating over the chamber was also calculated. *$p < 0.0001$, two-tailed unpaired Student's *t*-test. Data are shown as mean + SEM of three mice from one experiment representative of three performed. (D) Adoptive transfers of total spleen cells from *Myo1g*$^{-/-}$ and WT mice mixed at different proportions were done in WT recipient mice. These cells were previously marked with different concentrations of CFSE to identify them in spleens, lymph nodes, or blood by flow cytometry after mice sacrifice, 2 h later of its injection by the tail vein. The migrating transferred B cells were identified by its CFSE-staining level and B220 expression (top). The recovery ratios for each mix transferred as indicated in the graph are also shown (bottom). Data are shown as mean + SD of three mice in a single experiment representative of three performed in which the experimental mixes were *Myo1g*$^{-/-}$ cells and WT cells at the indicated proportions. The control mix (left side of panel) was WT cells only. Recovery ratios for the control mix were all close to 1.0 (dashed horizontal line). In the experimental mixes, the recovery ratio was decreased for *Myo1g*$^{-/-}$ B cells ($p < 0.05$) in all mixes assayed.

[31–34]. We could not detect any differences in the total production of prolactin and TNF-α in activated B lymphocytes (Supporting Information Figs. 2 and 3) but by measuring the secreted fraction of both molecules we found that Myo1g-deficient B cells displayed a reduction in the exocytosis of these proteins when compared with that by WT lymphocytes (Fig. 4D and E).

Discussion

It was previously reported that Myo1g is associated with the plasma membrane of lymphocytes through its TH1 region [13]. It has been also determined that microvilli of human T cells and those from a mouse pre-B-cell line are rich in Myo1g [35]. Microvilli are formed by central actin filament bundles that are connected to the overlying plasma membrane by several linking proteins, including class I myosin. These structures represent functional lymphocyte domains that allow molecule segregation, probably to mediate different cell–cell interactions [36]. Interestingly, microvilli of mature B cells are inducible. They are increased in number and length after stimulation with different stimuli such as IL-4, LPS, or anti-CD40 antibodies [36], thus relating the marked presence of microvilli with an activated phenotype of B lymphocytes.

The distribution observed for Myo1g is highly similar to that described for Myo1c, another class I myosin also expressed by B cells [18]. Interestingly, it has been reported that the divergence in sequences of the TH1 domains of these two myosins is related with changes in lipid-binding affinities [13]. In other experiments it has been shown the coexistence of different lipid rafts over the membrane of B lymphocytes that differ in ultrastructure, immersed proteins but most importantly, lipid composition [37, 38]. It is possible that Myo1g and Myo1c, although both expressed by B cells and located in the same structures, develop different functional roles according to their ability to be recruited to different compartments of plasma membrane [39, 40].

In an effort to expand our understanding of Myo1g function in B cells, we have analyzed a Myo1g-deficient mouse strain. *Myo1g*$^{-/-}$ mice did not exhibit any significant phenotype at the whole animal level. When we analyzed the spleen B lymphocyte fraction of these animals, we could not find significant changes in the major subpopulations (Supporting Information Fig. 4) neither in their activation properties or proliferation rate (Supporting Information Fig. 5) when compared with WT mice splenic B cells. Additionally, most of the freshly isolated B cells (resting) obtained either from WT or *Myo1g*$^{-/-}$ mice, expressed both IgD and IgM (Supporting Information Fig. 6) with no detectable surface CD69 (naïve phenotype).

As Myo1g is associated with microfilament cytoskeleton-dependent plasma membrane protrusions, we searched for a role of this motor protein in cytoskeleton rearrangements. Using our previously established model [18], we found that Myo1g-deficient B lymphocytes exhibited an altered spreading pattern that decreased the number and extension of long plasma-membrane protrusions.

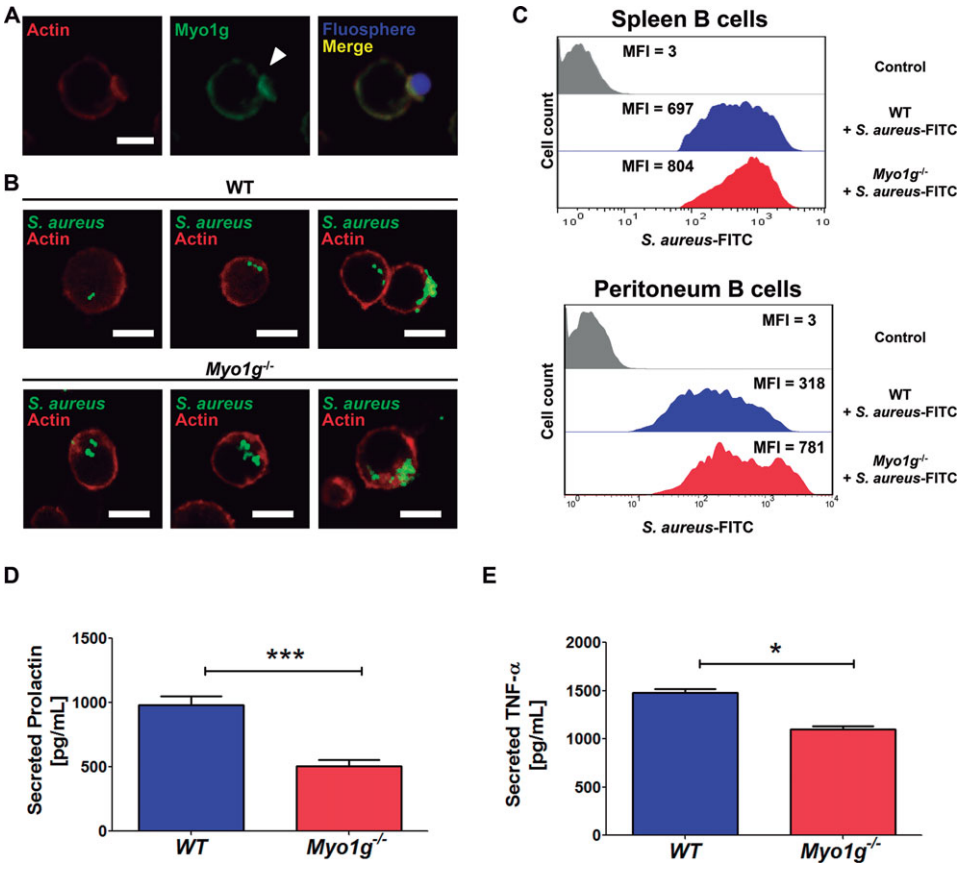

Figure 4. Altered phagocytosis and exocytosis in *Myo1g*$^{-/-}$ B cells. (A) Spleen-activated B cells were mixed 1:10 with 2 μm fluorescent polystyrene beads. After 1 h of incubation, the cells were collected and stained for F-actin and Myo1g detection in the phagocytic cups formed under the beads (white arrow). (B) Peritoneal B cells were "fed" with formalin-fixed FITC-labeled *Staphylococcus aureus*, in the same conditions that the beads previously used. These cells were collected, fixed, and stained with TRITC-phalloidin for F-actin before confocal microscopy analysis. Scale bars: 5 μm. (C) At the end of the phagocytosis experiment described in (B), the cells were treated with Trypan Blue to quench the fluorescence of noningested particles in order to determine only the amount of phagocytosed bacteria by flow cytometry. Histograms show the MFI of *Myo1g*$^{-/-}$ and WT spleen and peritoneal cells, gated on a B220^{+} population; the data are from a single experiment representative of four performed. (D, E) Spleen resting or activated B cells, from WT and *Myo1g*$^{-/-}$ mice, were cultured during 48 h before the collection of supernatants and cells to look for (D) prolactin or (E) TNF-α secretion by ELISA. $^{***}p < 0.0001$ or $^{*}p < 0.03$, two-tailed unpaired Student's *t*-test.

This behavior was previously observed in MyoC-deficient *Dictyostelium* amoebas which lack of the ability to generate directed pseudopodia [41]. In B cells, our group previously reported that down-regulation of Myo1c in B cells has the same effect [18]. A possible explanation for these observations is the membrane tension. Membrane tension is the loading force that growing actin filaments fight in order to protrude the membrane [30]. It was previously demonstrated that inhibiting the function of class I myosins function decreased the membrane tension in fibroblasts [42] and that down-regulation of Myo1g expression in T cells gives the same effect. According to this, it has also been observed that the decrease in membrane tension correlates with an increased protrusion generation in fibroblasts [43] and the uniform peripheral expansion of the leading edge and loss of polarity of migrating neutrophils. Taken together, these data suggest that the decreased membrane tension in Myo1g-deficient B cells could be responsible for the particular spreading pattern developed by these lymphocytes.

Additionally to the altered spreading, the Myo1g-deficient B cells (either unstimulated or activated) presented a diminished adhesive response over different substrates. It has been described that perturbation of cytoskeleton integrity and membrane tension immediately arrest cells in their regular spherical shape, thus abolishing spreading on the substrate [44]. Additionally, it has been observed in endothelial cell lines that the increase in membrane tension stimulate adhesion molecules aggregation favoring adhesive contacts between the cell surface and the substrate by bringing together both as a tension-induced membrane flattening occurs [45]. Accordingly, a decreased membrane tension in B cells due to Myo1g absence could be because of a misregulation in this adhesive process.

Another possible explanation for the adhesion defect in activated B cells emerged when we measured the surface levels of CD44 and LFA-1 integrin adhesion in these groups of lymphocytes. Although we found no significant differences in the total protein levels (Supporting Information Fig. 7), we detected a lower membrane expression of both molecules in activated Myo1g-deficient B cells. While it is still not clear if this phenotype could be the result of defects in the vesicular traffic pathways, we believe that the surface down-regulation of both molecules contributes to the adhesive defects of activated *Myo1g*$^{-/-}$ B cells.

The motility of the Myo1g-deficient B cells was also found altered. The *Myo1g*$^{-/-}$ B lymphocytes were slower and developed shorter trajectories upon stimulation with an agonist chemokine, CXCL13. Again, this behavior could be attributed to the reduced expression of adhesion molecules, which are involved in homing/recirculation processes in lymphocytes [46, 47]. As previously mentioned, the reduction of the membrane tension exerted by class I myosin deficiency likely impairs the polarization of the migrating B cells toward a chemokine gradient, thus slowing down their movement.

Moreover, class I myosins have been previously described as molecules that participate in processes such as phagocytosis and exocytosis [48]; consequently, we investigated the same activities in B cells.

It has been reported that certain class I myosins of *Entamoeba histolytica* control the initial steps of phagocytosis and are present and enriched in the phagocytic cups and phagosomes [49]. When we look for the presence of Myo1g in the phagocytic cups of activated B cells engulfing latex beads, we found this myosin enriched at these actin-dependent membrane structures.

When we measured the phagocytic rate of the *Myo1g*$^{-/-}$ spleen and peritoneal B lymphocytes, we observed an increased *Staphylococcus aureus*-FITC engulfment when compared with control cells. These data indicate that Myo1g-deficient B cells actually are more prone to phagocytosis which also could be explained in terms of membrane tension. It has been reported that a decreased in membrane tension correlates with an excess of endocytosis [50]. Additionally, it was shown that over-expression of myosin 1B in *Entamoeba histolytica* produced a decrease in phagocytosis [51], a fact that was attributed to an increase of cortical tension. Therefore, as it was formerly stated [50], a reduction in membrane tension increases endocytic processes; in contrast, it is also known that this same alteration concurrently reduces the exocytosis phenomena. As a result, we looked for defects in secreted molecules of B lymphocytes such as prolactin and TNF-α, both expressed by these cells upon activation [31–34].

Prolactin is a peptide hormone secreted by the anterior pituitary gland that is critical in lactation. This hormone has been characterized as an immune modulator of apoptosis, activation, and proliferation in leukocytes [31–33]. TNF-α is a well-known pro-inflammatory cytokine produced mainly by macrophages that can be also secreted by B cells [34].

As expected, we found a diminished TNF-α and prolactin secretion by *Myo1g*$^{-/-}$ B lymphocytes. This observation supports the idea that Myo1g controls the membrane tension in B cells, which is directly linked with the exocytosis/endocytosis pathways. These processes are also related with cytoplasmic vesicular traffic, which could also be altered by the Myo1g deficiency. Further studies are necessary to understand the role of Myo1g in cytoplasmic vesicular trafficking.

Material and methods

Mice

Female C57BL/6J and *Myo1g*$^{-/-}$ on a C57BL/6J genetic background (6–8 weeks of age) were used in all experiments. The mice were produced at Centro de Investigación y de Estudios Avanzados del Instituto Politécnico Nacional (CINVESTAV-IPN; México City, México) animal facility under specific pathogen-free conditions. The animal care and use committee of CINVESTAV-IPN approved all experiments.

Abs and reagents

Rabbit or goat polyclonal IgG anti-Myo1g, goat anti-actin, goat anti-calnexin, goat anti-lamin B (Santa Cruz), purified NIM-R8 (monoclonal rat anti-CD44), purified anti-LFA-1, and biotinylated mouse anti-CXCR5 (BD Biosciences), Alexa488 goat anti-rabbit IgG, HRP anti-rabbit IgG, and HRP-anti-goat IgG, TRITC-phalloidin, Pacific Blue anti-B220, FITC anti-LFA-1 (BD Pharmingen), DAPI, phalloidin-rhodamine (Molecular Probes), Cy3-streptavidin, allophycocyanin-streptavidin (Zymed), and recombinant mouse CXCL13 (Peprotech).

B lymphocyte isolation and activation

Spleen mononuclear cells were initially isolated by Ficoll-density gradient separation. B lymphocytes were then enriched by panning, using Petri dishes precoated with anti-Thy-1 ascites (containing NIM-R1 monoclonal antibodies). Purity of these lymphocytes was no less than 90%, measured by B220 expression by flow cytometry (Supporting Information Fig. 8). For activation purposes, 2×10^6 purified B lymphocytes were incubated in 1 mL 10% FBS supplemented RPMI 1640 (Life Technologies) supplemented with *Escherichia coli* O55:B5 LPS at 50 mg/mL (Sigma) plus 10 U/mL IL-4 (Genzyme) for 48 h at 37°C.

Microvilli separation and protein content analysis

Activated splenic B cells (1×10^9) were incubated in PBS containing 20% FBS for 20 min at 37°C. These lymphocytes were then carefully passed through a $27^{1/2}$G needle five times to shear off the microvilli from the cell surface. These samples were then fractionated as described previously [18, 35] for the separation of the MMV fraction and the PNL fraction. Both components were then analyzed by Western blot following conventional procedures.

Spreading assays and immunofluorescence staining

Glass slides or polystyrene-96 plates were coated with 20 μg/mL of NIM-R8 or anti-LFA-1 in PBS for 1 h at 37°C. The plates were blocked with PBS containing 10% FCS for 1 h at 37°C and then washed extensively with medium before use. Activated B cells were transferred without washing to the precoated glass slides or plates and were incubated for 1 h at 37°C. For confocal microscopy preparations, the cells were washed once with PBS and then fixed with 4% paraformaldehyde for 15 min. The cells were then washed again with PBS and then permeabilized with 0.1% of Triton X-100 in PBS for 10 min. After a final wash with PBS, the lymphocytes were incubated with different antibodies or fluorescent reagents, and mounted as described previously [18]. The obtained slides were observed with either Olympus or Leica microscopes using 60× objectives and NIH ImageJ or Olympus FluoView software for analysis.

Lipid raft isolation

For lipid raft isolation, purified B cells (1×10^8) were washed once with ice-cold PBS and lysed during 30 min at 4°C with 1% Triton X-100 in TNE buffer containing phosphatase and protease inhibitors (TNE: 10 mM Tris/HCl, pH 7.5, 150 mM NaCl, and 5 mM EDTA plus 2.5 mg/mL each of PMSF, leupeptin, aprotinin in DMSO) [18]. The lysate was then blended in with ten strokes of a Wheaton loose-fitting Dounce homogenizer. To clear the supernatant, cell debris and nuclei were separated by centrifugation during 10 min at 900 × *g*. For the discontinuous sucrose gradient preparation, 1 mL of 85% sucrose in TNE was mixed with 1 mL of cleared supernatant and carefully transferred to the bottom of a 14 × 95 mm centrifuge tube. This diluted lysate was carefully overlaid with 6 mL of 35% sucrose in TNE and finally 3.5 mL of 5% sucrose in TNE, avoiding mixing. The tubes were centrifuged during 20 h at 200 000 × *g* and 4°C. At the end, fractions of 1 mL were collected from the top of the tube and then analyzed by Western blot.

Adhesion assays

A total of 96-well polystyrene plates (Nalge Nunc International) were coated with various substrate molecules such as poly-L-Lysine (0.01%, Sigma), fibronectin (2.5 μg/mL, Takara), purified anti-CD44 or anti-LFA-1, during 1 h at 37°C. The plates were then washed twice with PBS before adding 4×10^5 panning-enriched B cells in 200 μL of RPMI 1640 per well. The cells were allowed to adhere for 1 h at 37°C. After that, the plates were washed with 300 μL of PBS, fixed with 4% paraformaldehyde for 10 min, before adding crystal-violet (crystal-violet 7·5 g/l, NaCl 2·5 g/l, formaldehyde 1·57%, methanol 50%) for an additional 5 min. The cells were washed extensively three times with distilled water, solubilized with 10% SDS, and the plates were read at 540 nm (Multiskan Ascent, Thermo Scientific, Waltham, MA). After subtraction of nonspecific colorimetric readings to obtain absolute binding, the absorbance for each well was registered, in at least four wells per condition, in three independent experiments.

In vitro chemotaxis assays

For quantification of migration, a Zigmond chamber (Neuroprobe) was used. Briefly, 1×10^6 B lymphocytes were suspended in 0.5 mL of 10% FBS supplemented RPMI 1640 (Life Technologies) and immediately plated onto glass coverslips, previously coated with 2.5 μg/mL of fibronectin (Takara), that were incubated for 30 min at 37°C and 5% CO_2 to allow the cells to attach. The coverslips, with the cells attached, were gently washed with 2.0 mL PBS, and 100 μL of supplemented RPMI 1640 was pipetted onto the coverslips, which in turn were placed upside-down onto the Zigmond slides and fixed. One of the grooves in the Zigmond chamber was filled with supplemented medium (approximately 80 μL) and the chamber was placed under a microscope. A baseline image was obtained at 40× magnification and the other groove was then filled with CXCL13 (50 μg) dissolved also in supplemented medium. Digital images of the cells were taken every 30 s for 1.5 h maintaining the temperature of the room between 35 and 39°C. For analyzing the trajectories and speed of migration, the migration tracks were traced for at least 100 lymphocytes of each genotype, in six independent experiments, using the NIH ImageJ software with chemotaxis and migration tool 2.0 (Ibidi).

In vivo homing assay

Ficoll-purified mononuclear cells from spleens of *Myo1g*$^{-/-}$ mice or control mice were labeled with either 0.1 μM (low concentration) or 0.6 μM (high concentration) CFSE (Invitrogen). The cells were mixed at a 1:1 ratio and injected via tail vein to recipient mice, 15×10^6 per mouse. The recipient mice were sacrificed 2 h after the adoptive transfer of labeled cells. Spleens and inguinal lymph nodes were excised and B lymphocytes were surface stained with PE-Cy7 conjugated anti-B220, (Biolegend). The cells were analyzed by a CyAn ADP flow cytometer (Beckman Coulter) for the presence of labeled cells and for B220 marker. Recovery ratios of each population were calculated as percentages using FlowJo software (Tree Star). To validate the procedure, in each experiment, control cells were labeled with both high and low concentrations of CFSE and injected. Ratio close to 1:1 of the high and low CFSE-labeled cells in the lymph nodes of the recipient mice indicates that the homing behavior of the cells was not differentially changed by the dye.

Phagocytosis assays

For in vitro assessment of phagocytosis, panning-enriched B cells or total peritoneal cells were incubated (1×10^6 cells per well) with FITC-labeled *S. aureus* (prepared as described in [52]) or polystyrene fluorescent microspheres (Molecular Probes) of 2 or 0.5 μm, at bacterium-to-cell or bead-to-cell ratio of 10:1 in 24-well plates in a volume of 500 μL of supplemented RPMI 1640 medium for 1 h at 37°C in 5% CO_2. The cells were then harvested and washed with PBS before the addition of 0.5 mL of a Trypan Blue solution (50 μg/mL) to quench the fluorescence of non-ingested particles by flow cytometry assays. After a brief incubation of 2 min, the dye was washed with PBS three times and the cells were subjected to fixation with 3.7% formaldehyde or Pacific Blue anti-B220 staining (only for the total peritoneal cell preparation) before fixation. Cell suspensions were then analyzed using a CyAn ADP flow cytometer (Beckman Coulter).

Analysis of exocytosis

A total of 2×10^6 cells/well panning-enriched spleen B cells from WT or *Myo1g*$^{-/-}$ mice were cultured in 24-well plates for 48 h. These were activated with LPS and IL-4 as described before. At

the end of the incubation period, supernatants were collected and analyzed for TNF-α or prolactin concentration by ELISA using conventional methods.

Statistical analysis

Results are presented as mean + SD. Unpaired two-tailed Student's *t*-test was used to assess statistical significance between two groups. The *p* values obtained and the number of samples or cells (*n*) used are mentioned in each corresponding figure legend.

Acknowledgments: We thank Steve Shaw from NCI, NIH for providing *Myo1g*$^{-/-}$ mice, Eduardo García-Zepeda for the CXCL13, Karina Chávez-Rueda and Araceli Pérez-López for the ELISA reagents, Rommel Chacón-Salinas for the anti-CXCR5, Maria Eugenia Mendoza-Garrido for the anti-prolactin, and Amanda M. Burkhardt and Tristan K. Zimmerman for the review of the manuscript. We also thank Héctor Romero-Ramírez and Julio García-Cordero for their help at different stages of this work. This work was supported by CONACyT (grant 153733). J.L.M.M. and O.L.O. were supported by fellowships 203768 and 219624 from CONACyT.

Conflict of interest: The authors declare no financial or commercial conflict of interest.

References

1 **Kim, S. V. and Flavell, R. A.**, Myosin I: from yeast to human. *Cell Mol. Life Sci.* 2008. **65**: 2128–2137.

2 **Berg, J. S., Powell, B. C. and Cheney, R. E.**, A millennial myosin census. *Mol. Biol. Cell* 2001. **12**: 780–794.

3 **Coluccio, L. M., Myosin I.** *Am. J. Physiol.* 1997. **273**: C347–C359.

4 **Albanesi, J. P., Fujisaki, H., Hammer, J. A., 3rd, Korn, E. D., Jones, R. and Sheetz, M. P.**, Monomeric Acanthamoeba myosins I support movement in vitro. *J. Biol. Chem.* 1985. **260**: 8649–8652.

5 **Stafford, W. F., Walker, M. L., Trinick, J. A. and Coluccio, L. M.**, Mammalian class I myosin, Myo1b, is monomeric and cross-links actin filaments as determined by hydrodynamic studies and electron microscopy. *Biophys. J.* 2005. **88**: 384–391.

6 **Coluccio, L. M., Mooseker, M. S. and Foth, B. J.**, *The Structural And Functional Diversity Of The Myosin Family Of Actin-Based Molecular Motors Myosins*. Springer, the Netherlands, 2008, pp. 1–34.

7 **Doberstein, S. K. and Pollard, T. D.**, Localization and specificity of the phospholipid and actin binding sites on the tail of Acanthamoeba myosin IC. *J. Cell Biol.* 1992. **117**: 1241–1249.

8 **Lee, W. L., Ostap, E. M., Zot, H. G. and Pollard, T. D.**, Organization and ligand binding properties of the tail of Acanthamoeba myosin-IA. Identification of an actin-binding site in the basic (tail homology-1) domain. *J. Biol. Chem.* 1999. **274**: 35159–35171.

9 **Heng, T. S. and Painter, M. W.**, The Immunological Genome Project: networks of gene expression in immune cells. *Nat. Immunol.* 2008. **9**: 1091–1094.

10 **Wu, C., Orozco, C., Boyer, J., Leglise, M., Goodale, J., Batalov, S., Hodge, C. et al.**, BioGPS: an extensible and customizable portal for querying and organizing gene annotation resources. *Genome Biol.* 2009. **10**: R130.

11 **Maravillas-Montero, J. L. and Santos-Argumedo, L.**, The myosin family: unconventional roles of actin-dependent molecular motors in immune cells. *J. Leukoc. Biol.* 2012. **91**: 35–46.

12 **Olety, B., Walte, M., Honnert, U., Schillers, H. and Bahler, M.**, Myosin 1G (Myo1G) is a haematopoietic specific myosin that localises to the plasma membrane and regulates cell elasticity. *FEBS Lett.* 2010. **584**: 493–499.

13 **Patino-Lopez, G., Aravind, L., Dong, X., Kruhlak, M. J., Ostap, E. M. and Shaw, S.**, Myosin 1G is an abundant class I myosin in lymphocytes whose localization at the plasma membrane depends on its ancient divergent pleckstrin homology (PH) domain (Myo1PH). *J. Biol. Chem.* 2010. **285**: 8675–8686.

14 **Dart, A. E., Tollis, S., Bright, M. D., Frankel, G. and Endres, R. G.**, The motor protein myosin 1G functions in FcgammaR-mediated phagocytosis. *J. Cell Sci.* 2012. **125**: 6020–6029.

15 **Lafourcade, C., Sobo, K., Kieffer-Jaquinod, S., Garin, J. and van der Goot, F. G.**, Regulation of the V-ATPase along the endocytic pathway occurs through reversible subunit association and membrane localization. *PLoS One* 2008. **3**: e2758.

16 **Linkermann, A., Gelhaus, C., Lettau, M., Qian, J., Kabelitz, D. and Janssen, O.**, Identification of interaction partners for individual SH3 domains of Fas ligand associated members of the PCH protein family in T lymphocytes. *Biochim. Biophys. Acta* 2009. **1794**: 168–176.

17 **Perez-Hernandez, D., Gutierrez-Vazquez, C., Jorge, I., Lopez-Martin, S., Ursa, A., Sanchez-Madrid, F., Vazquez, J. et al.**, The intracellular interactome of tetraspanin-enriched microdomains reveals their function as sorting machineries toward exosomes. *J. Biol. Chem.* 2013. **288**: 11649–11661.

18 **Maravillas-Montero, J. L., Gillespie, P. G., Patino-Lopez, G., Shaw, S. and Santos-Argumedo, L.**, Myosin 1c participates in B cell cytoskeleton rearrangements, is recruited to the immunologic synapse, and contributes to antigen presentation. *J. Immunol.* 2011. **187**: 3053–3063.

19 **Sumoza-Toledo, A., Gillespie, P. G., Romero-Ramirez, H., Ferreira-Ishikawa, H. C., Larson, R. E. and Santos-Argumedo, L.**, Differential localization of unconventional myosin I and nonmuscle myosin II during B cell spreading. *Exp. Cell Res.* 2006. **312**: 3312–3322.

20 **Soldati, T.**, Unconventional myosins, actin dynamics and endocytosis: a menage a trois? *Traffic* 2003. **4**: 358–366.

21 **Nebl, T., Pestonjamasp, K. N., Leszyk, J. D., Crowley, J. L., Oh, S. W. and Luna, E. J.**, Proteomic analysis of a detergent-resistant membrane skeleton from neutrophil plasma membranes. *J. Biol. Chem.* 2002. **277**: 43399–43409.

22 **Saeki, K., Miura, Y., Aki, D., Kurosaki, T. and Yoshimura, A.**, The B cell-specific major raft protein, Raftlin, is necessary for the integrity of lipid raft and BCR signal transduction. *EMBO J.* 2003. **22**: 3015–3026.

23 **Houk, A. R., Jilkine, A., Mejean, C. O., Boltyanskiy, R., Dufresne, E. R., Angenent, S. B., Altschuler, S. J. et al.**, Membrane tension maintains cell polarity by confining signals to the leading edge during neutrophil migration. *Cell* 2012. **148**: 175–188.

24 **Liu, Y., Belkina, N. V., Park, C., Nambiar, R., Loughhead, S. M., Patino-Lopez, G., Ben-Aissa, K. et al.**, Constitutively active ezrin increases membrane tension, slows migration, and impedes endothelial transmigration of lymphocytes in vivo in mice. *Blood* 2012. **119**: 445–453.

25 **Bertram, A., Zhang, H., von Vietinghoff, S., de Pablo, C., Haller, H., Shushakova, N. and Ley, K.**, Protein kinase C-theta is required for murine neutrophil recruitment and adhesion strengthening under flow. *J. Immunol.* 2012. **188**: 4043–4051.

26 **Ng, T., Parsons, M., Hughes, W. E., Monypenny, J., Zicha, D., Gautreau, A., Arpin, M. et al.**, Ezrin is a downstream effector of trafficking PKC-integrin complexes involved in the control of cell motility. *EMBO J.* 2001. **20**: 2723–2741.

27 **Popi, A. F., Zamboni, D. S., Mortara, R. A. and Mariano, M.**, Microbicidal property of B1 cell derived mononuclear phagocyte. *Immunobiology* 2009. **214**: 664–673.

28 **Gao, J., Ma, X., Gu, W., Fu, M., An, J., Xing, Y., Gao, T. et al.**, Novel functions of murine B1 cells: active phagocytic and microbicidal abilities. *Eur. J. Immunol.* 2012. **42**: 982–992.

29 **Ray, A. and Dittel, B. N.**, Isolation of mouse peritoneal cavity cells. *J. Vis. Exp.* 2010. **35**: e1488.

30 **Keren, K., Pincus, Z., Allen, G. M., Barnhart, E. L., Marriott, G., Mogilner, A. and Theriot, J. A.**, Mechanism of shape determination in motile cells. *Nature* 2008. **453**: 475–480.

31 **Buckley, A. R.**, Prolactin, a lymphocyte growth and survival factor. *Lupus* 2001. **10**: 684–690.

32 **Díaz, L., Díaz-Muñoz, M., González, L., Lira-Albarrán, S., Larrea, F. and Méndez, I.**, Prolactin in the Immune System. In Nagy, G.M. and Toth, B.E. (Eds.), *Prolactin*. InTech, Croatia, 2013.

33 **DiMattia, G. E., Gellersen, B., Bohnet, H. G. and Friesen, H. G.**, A human B-lymphoblastoid cell line produces prolactin. *Endocrinology* 1988. **122**: 2508–2517.

34 **Perez-Lopez, A., Rosales-Reyes, R., Alpuche-Aranda, C. M. and Ortiz-Navarrete, V.**, Salmonella downregulates Nod-like receptor family CARD domain containing protein 4 expression to promote its survival in B cells by preventing inflammasome activation and cell death. *J. Immunol.* 2013. **190**: 1201–1209.

35 **Hao, J. J., Wang, G., Pisitkun, T., Patino-Lopez, G., Nagashima, K., Knepper, M. A., Shen, R. F. et al.**, Enrichment of distinct microfilament-associated and GTP-binding-proteins in membrane/microvilli fractions from lymphoid cells. *J. Proteome Res.* 2008. **7**: 2911–2927.

36 **Greicius, G., Westerberg, L., Davey, E. J., Buentke, E., Scheynius, A., Thyberg, J. and Severinson, E.**, Microvilli structures on B lymphocytes: inducible functional domains? *Int. Immunol.* 2004. **16**: 353–364.

37 **Knorr, R., Karacsonyi, C. and Lindner, R.**, Endocytosis of MHC molecules by distinct membrane rafts. *J. Cell Sci.* 2009. **122**: 1584–1594.

38 **Petrie, R. J. and Deans, J. P.**, Colocalization of the B cell receptor and CD20 followed by activation-dependent dissociation in distinct lipid rafts. *J. Immunol.* 2002. **169**: 2886–2891.

39 **Greenberg, M. J. and Ostap, E. M.**, Regulation and control of myosin-I by the motor and light chain-binding domains. *Trends Cell Biol.* 2013. **23**: 81–89.

40 **Santos-Argumedo, L., Maravillas-Montero, J. L. and Lopez-Ortega, O.**, Class I myosins in B-cell physiology: functions in spreading, immune synapses, motility, and vesicular traffic. *Immunol. Rev.* 2013. **256**: 190–202.

41 **Peterson, M. D., Novak, K. D., Reedy, M. C., Ruman, J. I. and Titus, M. A.**, Molecular genetic analysis of myoC, a Dictyostelium myosin I. *J. Cell Sci.* 1995. **108**(Pt 3): 1093–1103.

42 **Nambiar, R., McConnell, R. E. and Tyska, M. J.**, Control of cell membrane tension by myosin-I. *Proc. Natl. Acad. Sci. USA* 2009. **106**: 11972–11977.

43 **Raucher, D. and Sheetz, M. P.**, Cell spreading and lamellipodial extension rate is regulated by membrane tension. *J. Cell Biol.* 2000. **148**: 127–136.

44 **Pietuch, A. and Janshoff, A.**, Mechanics of spreading cells probed by atomic force microscopy. *Open Biol.* 2013. **3**: 130084.

45 **Delanoe-Ayari, H., Al Kurdi, R., Vallade, M., Gulino-Debrac, D. and Riveline, D.**, Membrane and acto-myosin tension promote clustering of adhesion proteins. *Proc. Natl. Acad. Sci. USA* 2004. **101**: 2229–2234.

46 **Simon, S. I., Hu, Y., Vestweber, D. and Smith, C. W.**, Neutrophil tethering on E-selectin activates beta 2 integrin binding to ICAM-1 through a mitogen-activated protein kinase signal transduction pathway. *J. Immunol.* 2000. **164**: 4348–4358.

47 **Xu, H., Manivannan, A., Crane, I., Dawson, R. and Liversidge, J.**, Critical but divergent roles for CD62L and CD44 in directing blood monocyte trafficking in vivo during inflammation. *Blood* 2008. **112**: 1166–1174.

48 **Raposo, G., Cordonnier, M. N., Tenza, D., Menichi, B., Durrbach, A., Louvard, D. and Coudrier, E.**, Association of myosin I alpha with endosomes and lysosomes in mammalian cells. *Mol. Biol. Cell* 1999. **10**: 1477–1494.

49 **Marion, S., Laurent, C. and Guillen, N.**, Signalization and cytoskeleton activity through myosin IB during the early steps of phagocytosis in *Entamoeba histolytica*: a proteomic approach. *Cell Microbiol.* 2005. **7**: 1504–1518.

50 **Keren, K.**, Cell motility: the integrating role of the plasma membrane. *Eur. Biophys. J.* 2011. **40**: 1013–1027.

51 **Marion, S., Wilhelm, C., Voigt, H., Bacri, J. C. and Guillen, N.**, Overexpression of myosin IB in living *Entamoeba histolytica* enhances cytoplasm viscosity and reduces phagocytosis. *J. Cell Sci.* 2004. **117**: 3271–3279.

52 **Nibbering, P. H., Broug-Holub, E., Bezemer, A. C., Jansen, R., van de Winkel, J. G. and Geertsma, M. F.**, Phagocytosis and intracellular killing of serum-opsonized *Staphylococcus aureus* by mouse fibroblasts expressing human Fcgamma receptor type IIa (CD32). *Front Biosci.* 1996. **1**: a25–a33.

Abbreviations: **ATP**: adenosine triphosphate · **Myo1g**: myosin 1g · **MMV**: membrane/microvilli fraction · **PNL**: postnuclear lysate · **TH1**: tail homology 1

Full correspondence: Dr. Leopoldo Santos-Argumedo, Departamento de Biomedicina Molecular, Centro de Investigación y de Estudios Avanzados del IPN, Avenida IPN 2508, CP 07360, D.F., México
Fax: (+52-55)-57473938
e-mail: lesantos@cinvestav.mx

Current address: Genaro Patiño-López, Laboratorio de Investigación en Inmunología, Hospital Infantil de México, "Federico Gómez", CP 06720, Ciudad de México, México

Received: 3/7/2013
Revised: 22/10/2013
Accepted: 27/11/2013
Accepted article online: 5/12/2013

